99m Tc-labeled Duramycin for detecting and monitoring cardiomyocyte death and assessing cardioprotection of atorvastatin in acute myocardial infarction

Hui Tan
Zhongshan Hospital Fudan University
Mieradilijiang Abudupataer
Zhongshan Hospital Fudan University
Lin Qiu
Zhongshan Hospital Fudan University
Wujian Mao
Zhongshan Hospital Fudan University
Dengfeng Cheng
Zhongshan Hospital Fudan University
Hongcheng Shi (shihongcheng163@163.com)
Fudan University https://orcid.org/0000-0003-1922-1359

Original research

Keywords: duramycin, acute myocardial infarction (AMI), apoptosis, atorvastatin, SPECT/CT

Posted Date: February 17th, 2020

DOI: https://doi.org/10.21203/rs.2.23615/v1

Version of Record: A version of this preprint was published at Chemical Biology & Drug Design on September 3rd, 2020. See the published version at https://doi.org/10.1111/cbdd.13773.

Abstract

Background: The objective of this study was to evaluate the feasibility of dynamic monitoring of myocardial cell death using 99m Tc-Duramycin single photon emission computed tomography/computed tomography (micro-SPECT/CT) imaging in a mouse model of acute myocardial infarction, and the anti-apoptosis effect of atorvastatin for cardio protection.

Methods: Forty-five male Kunming mice were randomized into three groups: acute myocardial infarction (AMI) group, acute myocardial infarction with atorvastatin treatment (T-AMI) group, and the sham group. The mice of the AMI group and T-AMI group were subjected left coronary artery ligation. The T-AMI group was orally administered with atorvastatin 20 mg/ (kg day) 24 h before the surgery, the other two groups received only saline. Three groups of model mice were randomly selected at day 1 (D1), day 3 (D3), and day 7 (D7) day after surgery with 99m Tc-Duramycin micro-SPECT/CT imaging. Transthoracic echocardiography test was performed at D3 and D7 after surgery. The pathological evaluation, TUNEL assay and Western blot analysis were performed on heart specimens on D1, D3 and D7.

Results: For up-taking of 99m Tc-duramycin in infarcted region, the mean value of semi-quantitative of AMI group were 2.62 on D1, 3.89 on D3 and 1.20 on D7. And for the T-AMI group, the mean value of semi-quantitative were 2.20 on D1, 2.97 on D3 and 1.30 on D7. The sham group had no positive imaging in myocardium, the mean value of semi-quantitative were 1.09, 1.14 and 1.10 on D1, D3 and D7, respectively. Meanwhile, 99m Tc-linear-duramycin imaging as control showed that there's no radioactive uptake in the area of infarction region. But the T-AMI group imaging showed the tracer uptake decreased obviously compared to the uptake of AMI mice in infarcted region (L/N: 2.2 versus 2.62; 2.97 versus 3.89) on D3 and D7. LVEF was significantly reduced on D3 (42.67±2.51%) and D7 (27.71±2.52%) compared with the sham group (71.00±2.65%). The number of TUNEL positive cells decreased significantly on D3 (37.00±3.01 vs 51.00±3.61) and D7 (21.67±2.08 vs 27.65±2.51) post-MI after atorvastatin treatment. Additionally, the atorvastatin increased the expression level of anti-apoptotic protein BCL-2 and decreased the expression level of pro-apoptotic protein BAX.

Conclusions: 99m Tc-Duramycin SPECT/CT imaging allowed to the non-invasively monitoring of myocardial cell death in a mouse model of acute myocardial infarction. Furthermore, this investigation and analysis could be used to assess and verify the anti-apoptosis effect of atorvastatin for cardio protection by in-vivo molecular imaging.

Background

Acute myocardial infarction has become one of the leading causes of death in the world, and it has seriously endangered public health, there are roughly 32.4 million peoples suffers from this disease and strokes worldwide per year [1]. In acute myocardial infarction, complete obstruction of coronary artery leads to cell necrosis and apoptosis, which are the main cause of myocardial cell death in acute myocardial infarction. Early intervention inhibits myocardial cell apoptosis, which is beneficial to reduce

the infarct size and improve left ventricular function. Statins are hydroxymethylglutaric acid coenzyme reductase inhibitors, which have a significant lipid-lowering effect in the treatment of cardiovascular disease. Numerous studies showed that statins could effectively prevent apoptosis of myocardial cells in the infarcted area, reduce wall tension during diastole and reperfusion injury and myocardial ischemia, which may mechanistically attenuate myocardial apoptosis [2–4]. Therefore, it is pivotal that how to monitor myocardial cell death during myocardial infarction in vivo and evaluate the effects of statins and other anti-apoptotic drugs on myocardial infarction.

Currently, specific molecular targets for apoptosis include phospholipid eversion, caspase activation, altered mitochondrial permeability, FasR expression, and TNF mediated cell death [5, 6]. A vital sign of early cell apoptosis is the rapid eversion of phosphatidylserine (PS) and phosphatidylethanolamine (PE) exposed to the outer cell membrane, thus becoming a target for apoptotic molecular imaging. Studies have used Annexin V as a radiolabeled drug for apoptotic imaging [7–9]. Annexin V with a potent high-affinity for PS, is composed of 319 amino acids and has a molecular weight of 35.8 kDa. However, it has limitations with larger molecular weight resulting in slow clearance, and high blood and liver background [10]. Duramycin with molecular weight of 2 kDa, making up for these limitations, is a unique small molecule peptide containing 19 amino acids. It is an ideal target for detecting death including apoptosis and necrosis, which can specifically bind to PE with high affinity and low background [11].

Some studies had shown extensively application of ^{18}F or ^{99m}Tc labelled duramycin for detecting apoptosis in ischemia reperfusion injury, atherosclerosis, and tumors [12–16]. In this study, we evaluated the feasibility that the ^{99m}Tc-labeled duramycin used to monitor myocardial cell death in a mouse model of acute myocardial infarction. In addition, we further investigated its usefulness of cardioprotection assessment with the atorvastatin and verified anti-apoptosis effects by in-vivo molecular imaging.

Methods

Experimental animals and drugs

Forty-five male Kunming mice (age, 8-12 weeks; weight, 28-32 g) were provided by the Department of Animal Science of Shanghai Medical College of Fudan University. These mice were divided into three independent groups: AMI group, T-AMI group, and sham group. The left coronary artery of mice was ligated in the AMI group and T-AMI group [17]. The T-AMI group was orally administered with atorvastatin 20 mg/ (kg day) 24 h before the surgery, the other two groups received only saline. In the sham group all procedure was same as above the two groups but here coronary artery was not ligated. The protocol is summarized in Fig. 1. Current study was performed in strict accordance with the recommendations of the Guide for Animal Management Rules from the Ministry of Health of the People's Republic of China. The experimental protocols were approved by the medical ethics committee of Zhongshan Hospital, Fudan University and imitate to the Guide for Care and Use of Laboratory Animals.

Myocardial Infarction Model

Myocardial infarction (MI) was performed in the mice that described previously [17]. Here we briefly describe the whole procedure for the mice model for MI, mice were anesthetized with 1% isoflurane and placed supine position on the operating table. A disposable 22-G intravenous catheter was used to trachea cannulate and connect to a small animal ventilator to sustain the anesthesia. Before incision, hair are removed by applying hair remover cream over the chest and disinfect the whole area with 75% alcohol and finally 1 cm skin incision was cut along the left side of the sternum, then tweezers were used to split the fourth intercostal space into the chest and expose the heart. The left atrial appendage and ventricle were fully exposed, and the left anterior descending branch vessel (passed through the 1–2 mm below the tip of the left atrial appendage), was ligated with 8 − 0 suture. After successful ligation, the anterior wall of the heart below the ligation line quickly turned pale. The sham group mice had the same operation as stated above, but there are no ligation and ischemic injury to the mice. After ligation, no bleeding in the thorax was confirmed then close the thorax and finally stitched the skin with 4 − 0 sutures. Physical condition of mice was observed on daily basis.

Tc-99m Labeling Of Duramycin And Linear-duramycin

The procedure for Tc-99m labeling of duramycin was done according to the previously reported [18]. Single-step kit containing HYNIC-duramycin and HYNIC-linear duramycin were provided by Molecular Targeting Technologies, Inc., USA. Firstly, 300 μL of sodium acetate buffer (pH = 5.3) was added to single-step kit formulation, composed of 15 μg hydrazinonicotinamide (HYNIC)-duramycin for Tc-99m labeling. Secondly, in a 1.5-mL centrifuge tube, 50 μL (2.5 μg) HYNIC-duramycin solution and 100 μL freshly prepared [^{99m}Tc]-pertechnetate (185 MBq) was added, and then the mixture was inclubated at 80 °C for 20 min. The method of linear-duramycin was similar to that of Tc-99m labeling duramycin. The radiochemical purity of the probe was tested by using the high-performance liquid chromatography (HPLC).

Micro-SPECT/CT Imaging

Three groups of mice were randomly selected on day1 (D1), day3 (D3) and day7 (D7) after surgery for micro-SPECT/CT imaging, two mice selected in each group for each time point. These mice were injected with ^{99m}Tc-duramycin (18.5 MBq/0.5 μg per mouse) by a caudal vein. Furthermore, two mice from AMI group were selected on D3 after surgery and injected with [^{99m}Tc]-linear-duramycin. Three hours after injection, mice were placed into a micro-SPECT/CT scanner (Bioscan, Washington DC, USA) for imaging at mild anesthetic condition (2.2% isoflurane). The main parameters of SPECT were as follows: energy peak, 140 keV; window width, 10%; scanning time, 35 s/projection; matrix, 256 × 256; and resolution, 1 mm/pixel. The SPECT and CT images for mice were acquired at the same location. Data were reconstructed by the HiSPECT algorithm. The main parameters of CT were: tube current, 0.15 mA; tube

voltage, 45 keV; exposure time, 500 ms/frame; and frame resolution, 256 × 512. The protocol was displayed in Fig. 1.

The post-processing of data was performed with the software InVivo Scope (Version 1.43, Bioscan, Washington DC, USA). 3D region of interest (ROI) was drawn in left anterior descending region, while similar parameters were drawn in the site of normal myocardial tissue. We selected the lesion-to-normal myocardial tissue ratio (L/N) to express lesion signal intensity.

Echocardiography

Transthoracic echocardiography test was performed on D3 and D7 of post-myocardial infarction. Mice were anesthetized with 1% isoflurane and placed with supine position on the operating table. Using the Vevo770 imaging system (VisualSonics, Inc.), the left ventricular functions was quantified at the level of the papillary muscles to measure left ventricular ejection fraction (LVEF) at the same anatomic location in different mice. At least three consecutive beats were evaluated.

Histology And TUNEL Assay

The mice were anesthetized by 1% pentobarbital sodium injected subcutaneously. To remove the blood from the heart, the right atrial appendage was cut, normal saline and 4% neutral formaldehyde were sequentially perfused at the apex part of the heart. After the removing of blood, the heart was harvested and were fixed with 10% formalin (Well Biotech) for the paraffin embedding. H&E staining was performed in paraffin embedding tissues. For TdTmediated dUTP Nick-End Labeling (TUNEL) examination, hearts were fixed with 4% paraformaldehyde for 6-12 hours and incubated overnight in 30% sucrose to prepare frozen tissue. A TUNEL kit (Roche) was used to perform the assay. According the manufacturer's instructions, TdT and dUTP were mixed at a ratio of 1:9 as for working solution. The tissue section was covered by working solution and incubated in a 37 °C incubator for 2 h. Then the slices were washed with PBS for three times. After removing PBS, DAPI dye solution (Abcam) was added to the tissue and incubated for 10 min and observed under the fluorescence microscope (Leica). The entire procedures were performed at dark condition.

Western Blot Analysis

Heart tissues were cut into pieces and add moderate RIPA lysis buffer (Beyotime Biotechnology) and then the tissues were homogenized by ultrasonication by applying three cycles of 3 sec each of ultrasound. After homogenization, samples were put on lysis for 45 min at 4℃. After that, the lysed tissues were centrifuged at 14000 g for 25 minutes and the supernatant was collected. The protein concentration in the supernatant fraction was calculated by using BCA protein assay kit (Beyotime Biotechnology). Equivalent masses of proteins were diluted in sample loading buffer and heated for 5 minutes at 95℃.

Proteins were running on a 10% SDS–polyacrylamide gel and transferred onto polyvinylidene difluoride membranes. Membranes were then incubated with primary antibodies in a dilation of 1:1000: GAPDH (ab8245, Abcam), BCL-2 (Cell Signaling), BAX (Cell Signaling). Then, the membranes were incubated with a 1:6000 dilution goat anti-rabbit secondary antibodies (Biotech Well) for 1 hour at room temperature. Bands were detected by the Super Signal chemiluminescence reagent substrate (Millipore), and quantitative estimation of the bands' intensity was performed by using Image J software.

Statistical analysis

Three mice per group were used for the histological analyses of protein and the results are expressed as the mean ± SD. Statistical analysis was performed by GraphPad Prism 6 software. Two-tailed Student's t tests were used to compare two groups, and one-way ANOVA followed by Tukey's posthoc test was used for the comparison between two groups or more. Differences were considered significant at $P < 0.05$.

Results

Establishment of animal models

Forty-five male Kunming mice were used to establish an AMI or sham model. The design diagram of this study was illustrated in Fig. 1. Four mice died immediately after ligation of the anterior descending coronary artery, three of them caused by hemorrhagic shock due to a deep puncture of the heart during the needle insertion, and one of them caused accidentally touched a blood vessel during extrusion of the heart. One mouse of each AMI and T-AMI group was died on the second day of the operation, and two mice of AMI group died on the third day after the operation.

Results Of M-mode Echocardiography

To evaluate the success of the AMI model, LVEF was measured with two-dimensional, high-resolution echocardiography on D3 and D7. Representative echocardiographic images of infarcted heart of each group on D3 and D7 (Fig. 2A). LVEF was significantly reduced at D3 (42.67 ± 2.51%) and D7 (27.71 ± 2.52%) compared with the sham group (71.00 ± 2.65%) (Fig. 2B), indicating that the AMI model was successfully established.

In Vivo Micro-SPECT/CT

Radiochemical purity of ^{99m}Tc-duramycin was 96–98%, as analyzed by radio-HPLC. In vivo micro-SPECT/CT imaging showed the ^{99m}Tc-duramycin mainly accumulated in the area of kidneys and bladder, but the liver and myocardial background showed low uptake after 3-hour injection. ^{99m}Tc-duramycin uptake allowed noninvasive visualization for myocardial necrosis, and had no positive imaging in myocardium with visual analysis (Fig. 3). The results of semi-quantitative SPECT/CT, expressed as

lesion-to-normal myocardial tissue ratio (L/N), also showed that the uptake of myocardial death in AMI group had significantly higher radioactivity than sham group on D1 (L/N: 2.62 versus 1.09) and D3 (L/N: 3.89 versus 1.14). The mean value of semi-quantitative in sham group were 1.09 on D1, 1.14 on D3 and 1.10 on D7. Furthermore, there wasn't radioactive uptake in the area of infarction region from the ^{99m}Tc-linear-duramycin imaging (Fig. 4).

Moreover, the uptake of ^{99m}Tc-duramycin in the myocardial infarction area reached at peak on D3 in both AMI group and T-AMI group. There was just little uptake of ^{99m}Tc-duramycin in infarcted region on D7. For the up-taking of ^{99m}Tc-duramycin in infarcted region, the mean value of semi-quantitative analysis in AMI and T-AMI group were (2.62, 3.89 and 1.20) and (2.20, 2.97 and 1.30) at D1, D3 and D7, respectively after MI. Based on the visual analysis, we found that the tracer uptake was lower in T-AMI group mice in infracted region at D1 (L/N: 2.2 versus 2.62) than that of AMI group mice at. D3 (L/N: 2.97 versus 3.89).

Histological Evaluation

Morphological analysis of infarcted myocardium on D1, D3 and D7 post-injury was performed using H&E staining (Fig. 5). Many immune cells, necrotic myocardial cells, loss of muscle fiber integrity and fibrosis were observed on D1, D3 and D7 compared to those in sham group. From the Fig. 5 it was also observed that more extent of damage in AMI group at D3 as more numbers of immune cells and necrotic myocardial cells were compare to other two groups.

Apoptotic Evaluation

To evaluate the apoptosis in the infarcted heart tissue, to check the expression level of apoptosis related protein BCL-2 and BAX TUNEL staining assay and Western blot were performed on D1, D3 and D7 of post-injury. The representative TUNEL staining images of infarcted heart for the mice on D1, D3 and D7 were shown in Fig. 6A. Quantitation of TUNEL$^+$ cells in infarcted heart of each group was also shown in Fig. 6B. TUNEL staining assay showed that MI induced the apoptosis of the myocardial cells, and TUNEL$^+$ cells reached to the peak on D3 after MI. In addition to these analyses, expression level of anti-apoptotic protein BCL-2 and pro-apoptotic protein was also estimated by using Western blot (Fig. 6C) Western blot image showed there is upregulation of pro-apoptotic protein and downregulation of anti-apoptotic BCL-2 protein in the infarcted heart samples of AMI group mice on D1, D3 and D7 post-MI whereas reversed order was observed in T-AMI group mice at respective days after MI (Fig. 6C). Protein level of BCL-2 and BAX in infarcted heart samples of mice on D1, D3 and D7 were quantified by Image J software and the result was shown in Fig. 6D. As same as the TUNEL result, it found that MI increases the expression of pro-apoptotic protein BAX and decreased the expression of anti-apoptotic protein BCL-2.

Atorvastatin Decreases The Myocardial Apoptosis After Myocardial Infarction

The mice were treated with atorvastatin after myocardial infarction. LVEF was significantly increased on D3 (50.00 ± 2.10% vs 42.67 ± 2.51%) and D7 (37.33 ± 2.23% vs 27.71 ± 2.52%) compared to sham group after MI (Fig. 2). H&E staining showed that treatment of atorvastatin attenuated the myocardial injury after MI with the decreasing number of immune cells and necrotic myocardial cells (Fig. 5). Furthermore, the number of TUNEL positive cells decreased significantly on D3 (37.00 ± 3.01 vs 51.00 ± 3.61) and D7 (21.67 ± 2.08 vs 27.65 ± 2.51) post-MI after atorvastatin treatment (Fig. 6B). Additionally, atorvastatin increased the expression level of anti-apoptotic protein BCL-2 and decreased the expression level of pro-apoptotic protein (Fig. 6C). These data illustrated that atorvastatin attenuated the dysfunction of infarcted myocardium by its anti-inflammatory and anti-apoptotic effect, as shown in Fig. 6.

Discussion

After the coronary artery occlusion, ischemia and hypoxia of myocardial cell lead to substantial myocardial cell death, including apoptosis and necrosis, following with changes in ventricular structure and function, and eventually result in heart failure [19]. In this study, a mouse model of acute myocardial infarction was successfully established by ligating the left anterior descending coronary artery, cardiac function was evaluated with echocardiography.

when cardiomyocytes are damaged, phospholipids of damaged cell membranes can be sensitive targets to detect cell death [20, 21]. In acute myocardial ischemia, cardiomyocytes will undergo apoptosis and necrosis, and phospholipid proteins including PE and PS are the ectropion of the surface of the cell membrane. The cell membrane eversion of each apoptotic and necrotic cell can provide a rich of phospholipid protein binding sites [22–24]. Our previous research results showed that ^{99m}Tc-duramycin has higher specificity and affinity for apoptotic cells, lower blood background signals by comparing with ^{99m}Tc-Annexin V [11]. Studies displayed that mammalian cell membranes with abundant PE, was 5–6 times number with regard to that of PS [25]. Therefore, this study selected ^{99m}Tc-duramycin imaging to monitor the myocardial cell death in acute myocardial injury. The results revealed that ^{99m}Tc-duramycin imaging had radioactive concentration in the myocardial infarction area of the model (AMI and T-AMI) group, but no significant radioactive concentration in the corresponding sham group. In addition, ^{99m}Tc-linear-duramycin imaging showed no radioactive uptake in the area of infarction region, confirming ^{99m}Tc-duramycin specific uptake. Although the result of this study was similar to other findings, where the ^{99m}Tc-duramycin is predominantly excreted through the urinary system with relatively low systemic and hepatic background in its mouse model [13, 26]. Hence, this study indicated that ^{99m}Tc-duramycin enabled the detection of myocardial cell death effectively. These in vivo properties suggest that ^{99m}Tc-duramycin is a suitable molecular imaging agent for kinds of diseases in the cardiovascular system.

Regardless of the AMI group or the T-AMI group, the uptake of ^{99m}Tc-duramycin in the myocardial infarction area reached the peak on the third day after surgery. There was little uptake of ^{99m}Tc-duramycin in infarcted region on D7 after MI. The pathological H&E staining results showed that the area of myocardial death was the largest on D3 after myocardial infarction, compared with that on D1 and D7. Similarly, the result of the TUNEL staining assay also displayed that most apoptotic fluorescent staining signal was found on D3. To some extent, the pathology and imaging results were consistent, which revealed that ^{99m}Tc-duramycin imaging in vivo dynamic monitoring of myocardial cell death in acute myocardial injury is feasible. However, some studies have shown that myocardial apoptosis is most prominent on D1 after myocardial infarction [27, 28]. The possible cause is that ^{99m}Tc-duramycin imaging cannot recognize apoptosis and necrosis. Regardless of myocardial cell apoptosis and necrosis, phospholipid proteins including PE can be valgus to the outside of the cell membrane for bind ^{99m}Tc-duramycin.

Both AMI animal models and humans showed increased myocardial apoptosis in myocardial infarction, with BAX protein up-regulation and BCL2 protein down-regulation [29, 30]. Therefore, it is suggested that inhibition of apoptosis is an effective method to prevent myocardial infarction. Statins can reduce cardiomyocyte apoptosis by reducing the expression of TNF-α, and TRB3 in myocardial cells, inhibit ventricular remodeling after AMI, and improve cardiac function [4, 31–32]. In this study, the radioactive concentration signal of the ^{99m}Tc-duramycin imaging in the statin treatment group was lower than that in the corresponding AMI group by visual analysis. The T-AMI group showed decreased tracer uptake compared to AMI mice in infarcted region at D1 (L/N: 2.2 versus 2.62) and D3 (L/N: 2.97 versus 3.89). This suggests that the number of myocardial deaths in the mice of T-AMI group was less than that in the corresponding AMI group. Further, the results of pathological and TUNEL assay were also verified by the imaging results, that the MI range of T-AMI group is less than that of AMI group. BCL-2 can inhibit apoptosis, while promotes apoptosis. In this study, we also found that atorvastatin intervention can reduce the death of myocardial cells after myocardial infarction, with up-regulate the anti-apoptotic molecule BCL-2 and down-regulate the pro-apoptotic BAX protein. The results displayed that ^{99m}Tc-duramycin imaging can be applied to the evaluation of the efficacy of atorvastatin in the treatment of myocardial infarction. This will provide powerful imaging guidance for in vivo evaluating new drugs for treating myocardial infarction in the future.

A limitation of this study is impossible to realize a one-to-one comparison analysis between imaging results and pathological results and TUNEL assay. In this study, ^{99m}Tc-duramycin imaging was applied to continuous dynamic monitoring of myocardial cell death in myocardial infarction. Mice couldn't be sacrificed on D1 and D7. Other mice in the same group at the corresponding time point had no choice but to select for pathological analysis and TUNEL assay.

Conclusions

This study demonstrated that ^{99m}Tc-Duramycin SPECT/CT imaging allowed for non-invasively monitoring myocardial cell death in a mouse model of acute myocardial infarction. Furthermore, this investigation and analysis could be used to assess and verify anti-apoptotic effect of atorvastatin for cardioprotection by in vivo molecular imaging.

Abbreviations

SPECT/CT: Single photon emission computed tomography/computed tomography ; D1: Day 1; D3: Day 3; D7: Day 7; AMI: Acute myocardial infarction; T-AMI: Acute myocardial infarction with atorvastatin treatment; PS: Phosphatidylserine; PE: Phosphatidylethanolamine; MI: Myocardial infarction; HYNIC: hydrazinonicotinamide; HPLC: High-performance liquid chromatography; ROI: Region of interest; L/N: Lesion-to-normal myocardial tissue ratio; LVEF: Left ventricular ejection fraction; TUNEL: TdTmediated dUTP Nick-End Labeling ; WB: Western Blot; Echo: Echocardiography

Declarations

Ethics approval and consent to participate

The animal research protocol was approved by the Ethical Committee for Animal Research of Zhongshan Hospital, Fudan University. All the experiments were performed in accordance with the relevant guidelines and regulations of Fudan University.

Consent for publication

No applicable.

Availability of data and materials

The datasets generated and analyzed during this study are not publicly available due to all the data come from our prospective study.

Conflicts of interest

The authors declared that they have no conflicts of interest.

Funding

The authors acknowledge the funding from National Natural Science Foundation of China (No. 81901796, 81671735 and 81871407), and Shanghai Sailing Program Supported by Shanghai Science and Technology Commission (No. 19YF1408300).

Authors' contributions

H.T. and M. A. participated in the experimental and data analysis, and edited the main manuscript text. L.Q. and W.J.M. helped in synthesizing the probe and involved in animal imaging. H.T, D.F.C. and H.C.S. conceived and designed as well as controlled the quality of this study. All authors provided final approval of the version submitted for publication.

Acknowledgments

We are grateful to the nuclear medicine technologists Prof. Shaoli Song, Yingjian Zhang and Dr. Jianping Zhang from Center for Biomedical Imaging, Fudan University, and Shanghai Engineering Research Center of Molecular Imaging Probes.

References

1.GBD 2017 DALYs and HALE Collaborators. Global, regional, and national disability-adjusted life-years (DALYs) for 359 diseases and injuries and healthy life expectancy (HALE) for 195 countries and territories, 1990-2017: a systematic analysis for the Global Burden of Disease Study 2017. Lancet. 2018; 392:1859-922.

2.Huang P, Wang L, Li Q, Tian X, Xu J, Xu J, et al. Atorvastatin enhances the therapeutic efficacy of mesenchymal stem cells derived exosomes in acute myocardial infarction via up-regulating long non-coding RNA H19. Cardiovasc Res. 2020; 116:353-67.

3.Luo KQ, Long HB, Xu BC. Reduced apoptosis after acute myocardial infarction by simvastatin. Cell Biochem Biophys. 2015; 71:735-40.

4.Cheng WP, Lo HM, Wang BW, Chua SK, Lu MJ, Shyu KG. Atorvastatin alleviates cardiomyocyte apoptosis by suppressing TRB3 induced by acute myocardial infarction and hypoxia. J Formos Med Assoc. 2017; 116:388-97.

5.Zeng W, Wang X, Xu P, Liu G, Eden HS, Chen X. Molecular imaging of apoptosis: from micro to macro. Theranostics. 2015; 5:559-82.

6.Shekhar A, Heeger P, Reutelingsperger C, Arbustini E, Narula N, Hofstra L, Bax JJ, et al. Targeted imaging for cell death in cardiovascular disorders. JACC Cardiovasc Imaging. 2018; 11:476-93.

7.Belhocine TZ, Blankenberg FG, Kartachova MS, Stitt LW, Vanderheyden JL, HoebersFP, et al. (99m) Tc-Annexin A5 quantification of apoptotic tumor response: a systematic review and meta-analysis of clinical imaging trials. Eur J Nucl Med Mol Imaging. 2015; 42:2083-97.

8.Todica A, Zacherl MJ, Wang H, Böning G, Jansen NL, Wängler C, et al. In-vivo monitoring of erythropoietin treatment after myocardial infarction in mice with [□□Ga] Annexin A5 and [¹□F] FDG PET. J Nucl Cardiol. 2014; 21:1191-9.

9.Lu C, Jiang Q, Hu M, Tan C, Yu H, Hua Z. Preliminary biological evaluation of ¹⁸F-FBEM-Cys-Annexin V a novel apoptosis imaging agent. Molecules. 2015; 20:4902-14.

10.Wuest M, Perreault A, Richter S, Knight JC, Wuest F. Targeting phosphatidylserine for radionuclide-based molecular imaging of apoptosis. Apoptosis. 2019; 24:221-44.

11.Hu Y, Liu G, Zhang H, Li Y, Gray BD, Pak KY, et al. A Comparison of [^{99m}Tc] Duramycin and [^{99m}Tc] Annexin V in SPECT/CT Imaging Atherosclerotic Plaques. Mol Imaging Biol. 2018; 20:249-59.

12.Li Y, Liu C, Xu X, Lu X, Luo J, Gray B, et al. [^{99m}Tc] Tc-duramycin, a potential molecular probe for early prediction of tumor response after chemotherapy. Nucl Med Biol. 2018; 66:18-25.

13.Wang L, Wang F, Fang W, Johnson SE, Audi S, Zimmer M, et al. The feasibility of imaging myocardial ischemic/reperfusion injury using (99m) Tc-labeled duramycin in a porcine model. Nucl Med Biol. 2015; 42:198-204.

14.Audi SH, Jacobs ER, Zhao M, Roerig DL, Haworth ST, Clough AV. In vivo detection of hyperoxia-induced pulmonary endothelial cell death using (99m) Tc-duramycin. Nucl Med Biol. 2015; 42:46-52.

15.Delvaeye T, Wyffels L, Deleye S, Lemeire K, Gonçalves A, Decrock E, et al. Noninvasive whole-body imaging of phosphatidylethanolamine as a cell death marker using ^{99m}Tc-duramycin during TNF-induced SIRS. J Nucl Med. 2018; 59:1140-5.

16.Liu Z, Larsen BT, Lerman LO, Gray BD, Barber C, Hedayat AF, et al. Detection of atherosclerotic plaques in ApoE-deficient mice using (99m) Tc-duramycin. Nucl Med Biol. 2016; 43:496-505.

17.Tarnavski O, McMullen JR, Schinke M, Nie Q, Kong S, Izumo S. Mouse cardiac surgery: comprehensive techniques for the generation of mouse models of human diseases and their application for genomic studies. Physiol Genomics. 2004; 16:349-60.

18.Elvas F, Vangestel C, Rapic S, Verhaeghe J, Gray B, Pak K, et al. Characterization of [(99m) Tc] Duramycin as a SPECT imaging agent for early assessment of tumor apoptosis. Mol Imaging Biol. 2015; 17:838-47.

19.Hashmi S, Al-Salam S. Acute myocardial infarction and myocardial ischemia-reperfusion injury: a comparison. Int J Clin Exp Pathol. 2015; 8:8786-96.

20.Emoto K, Toyama-Sorimachi N, Karasuyama H, Inoue K, Umeda M. Exposure of phosphatidylethanolamine on the surface of apoptotic cells. Exp Cell Res. 1997; 232:430-4.

21.Hanshaw RG, Smith BD. New reagents for phosphatidylserine recognition and detection of apoptosis. Bioorg Med Chem. 2005; 13:5035-42.

22.Yuan G, Liu S, Ma H, Su S, Wen F, Tang X, et al. Targeting phosphatidylethanolamine with fluorine-18 labeled small molecule probe for apoptosis imaging. Mol Imaging Biol. 2019; doi: 10.1007/s11307-019-01460-0.

23.Elvas F, Stroobants S, Wyffels L. Phosphatidylethanolamine targeting for cell death imaging in early treatment response evaluation and disease diagnosis. Apoptosis. 2017; 22(8):971-87.

24.Wu JC, Qin X, Neofytou E. Radiolabeled duramycin: promising translational imaging of myocardial apoptosis. JACC Cardiovasc Imaging. 2018; 11:1834-6.

25.Post JA, Verkleij AJ, Langer GA. Organization and function of sarcolemmal phospholipids in control and ischemic/reperfused cardiomyocytes. J Mol Cell Cardiol. 1995; 27:749-60.

26.Kawai H, Chaudhry F, Shekhar A, Petrov A, Nakahara T, Tanimoto T, et al. Molecular imaging of apoptosis in ischemia reperfusion injury with radiolabeled duramycin targeting phosphatidylethanolamine: effective target uptake and reduced nontarget organ radiation burden. JACC Cardiovasc Imaging. 2018; 11:1823-33.

27.Anversa P, Cheng W, Liu Y, Leri A, Redaelli G, Kajstura J. Apoptosis and myocardial infarction. Basic Res Cardiol. 1998; 93 3:8-12.

28.Kajstura J, Cheng W, Reiss K, Clark WA, Sonnenblick EH, Krajewski S, et al. Apoptotic and necrotic myocyte cell deaths are independent contributing variables of infarct size in rats. Lab Invest. 1996; 74:86-107.

29.Misao J, Hayakawa Y, Ohno M, Kato S , Fujiwara T , Fujiwara H. Expression of bcl-2 protein, an inhibitor of apoptosis, and Bax, an accelerator of apoptosis, in ventricular myocytes of human hearts with myocardial infarction. Circulation. 1996; 94:1506-12.

30.Wu P, Du Y, Xu Z, Zhang S, Liu J, Aa N, et al. Protective effects of sodium tanshinone IIA sulfonate on cardiac function after myocardial infarction in mice. Am J Transl Res. 2019; 11:351-60.

31.Zhou L, Liu X, Wang ZQ, Li Y, Shi MM, Xu Z, et al. Simvastatin treatment protects myocardium in noncoronary artery cardiac surgery by inhibiting apoptosis through miR-15a-5p targeting. J Cardiovasc Pharmacol. 2018; 72:176-85.

32.Scalia R. Statins and the response to myocardial injury. Am J Cardiovasc Drugs. 2005; 5:163-70.

Figures

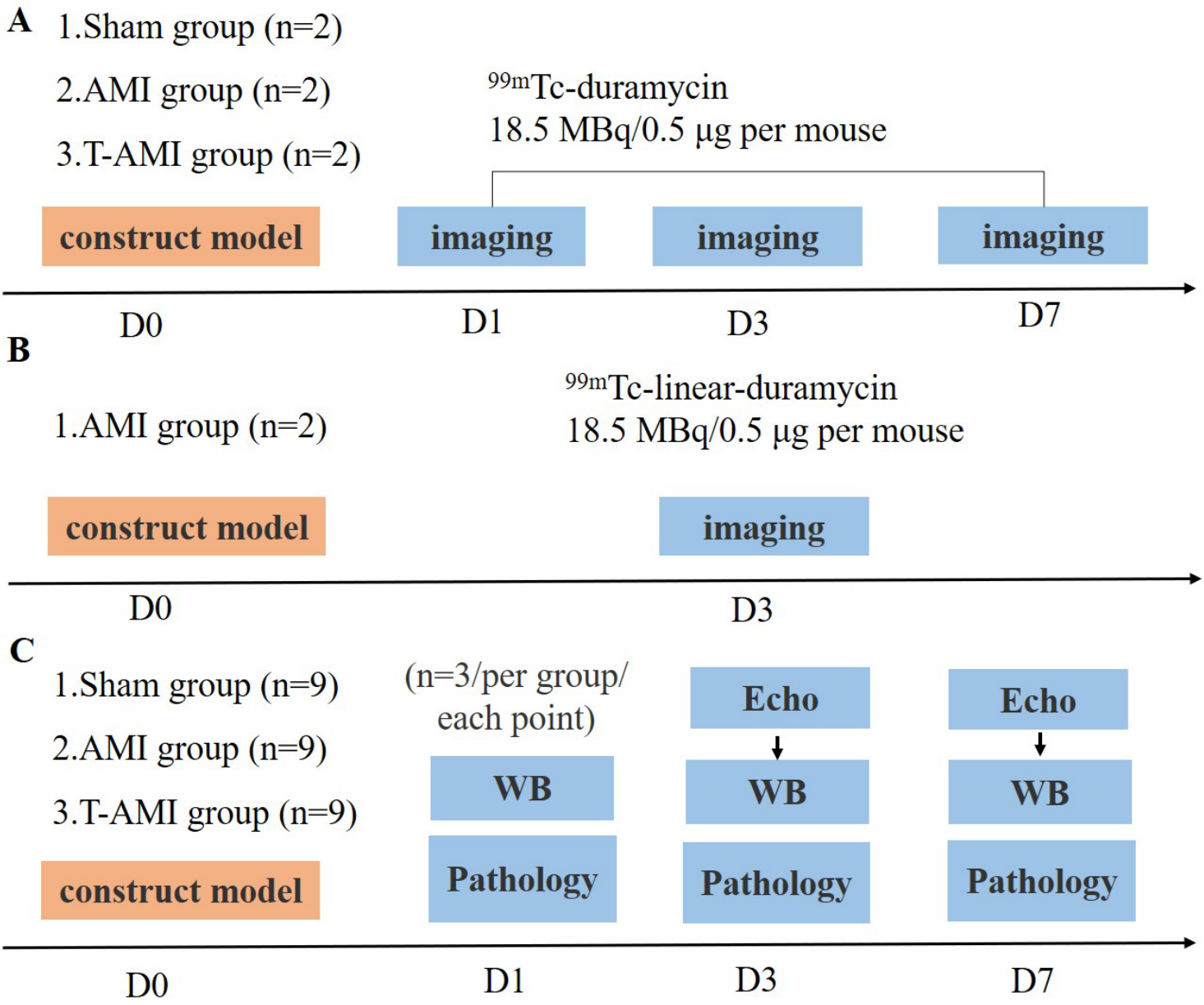

Figure 1

Study design flow chart.

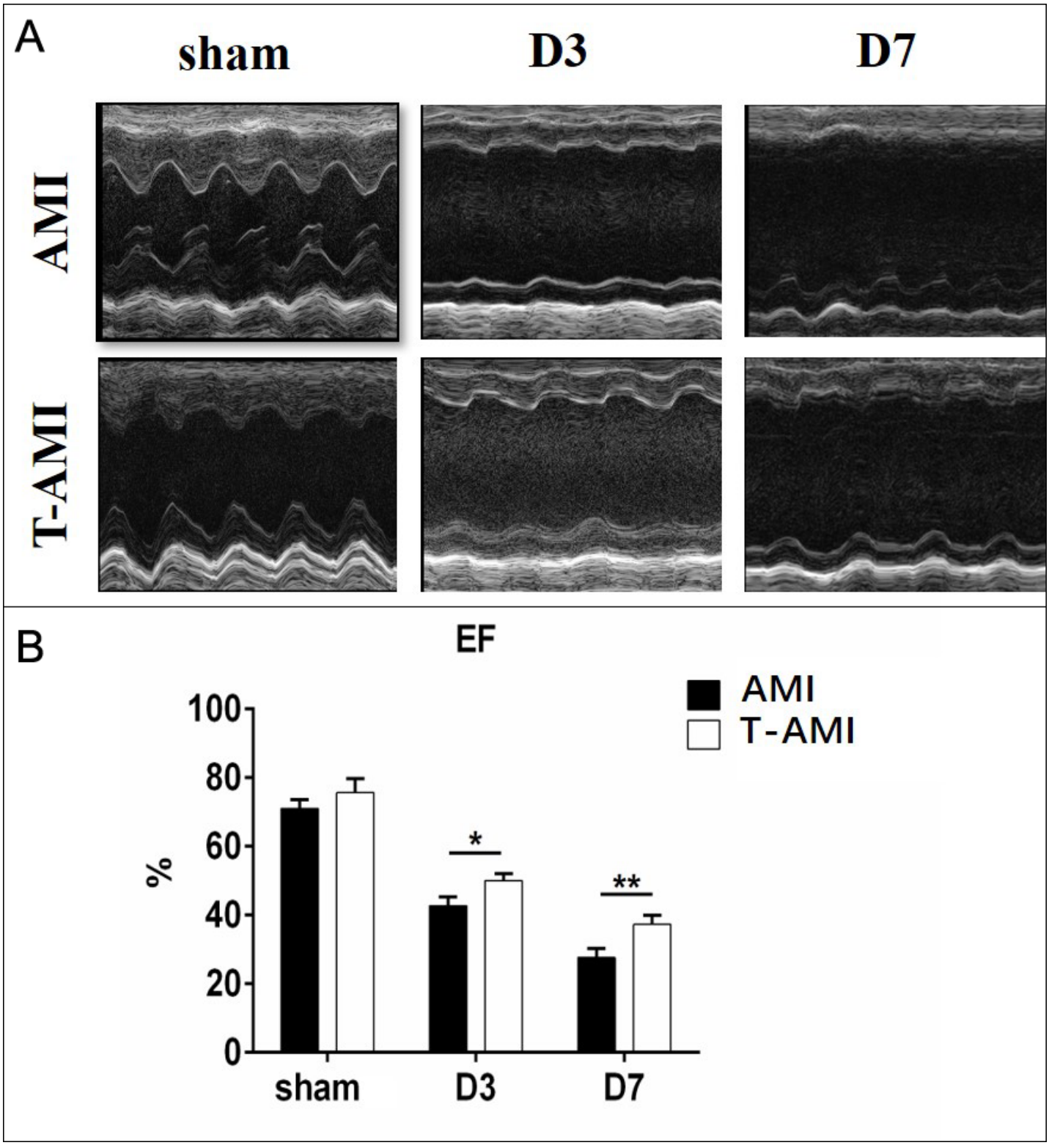

Figure 2

Assessment of myocardial function after myocardial infarction by M-mode echocardiography. (A) Representative echocardiographic images of infarcted heart of the AMI and T-AMI group mice on D3 and D7. (B) Quantitation of LVEF of the AMI, T-AMI and sham group mice on 3 days and 7 days after ligation. LVEF was significantly reduced on D3 (42.67±2.51%) and D7 (27.71±2.52%) compared with the sham group (71.00±2.65%), $p \leq 0.01$. Atorvastatin treatment significantly increased LVEF level on D3

(50.00±2.10% vs 42.67±2.51%, p ≤ 0.05) and D7 (37.33±2.23% vs 27.71±2.52%, p ≤ 0.01) compared with AMI group after MI. *P < 0.05, **P < 0.01, ***P < 0.001, ****P < 0.0001, error bars represent the mean ± SD.

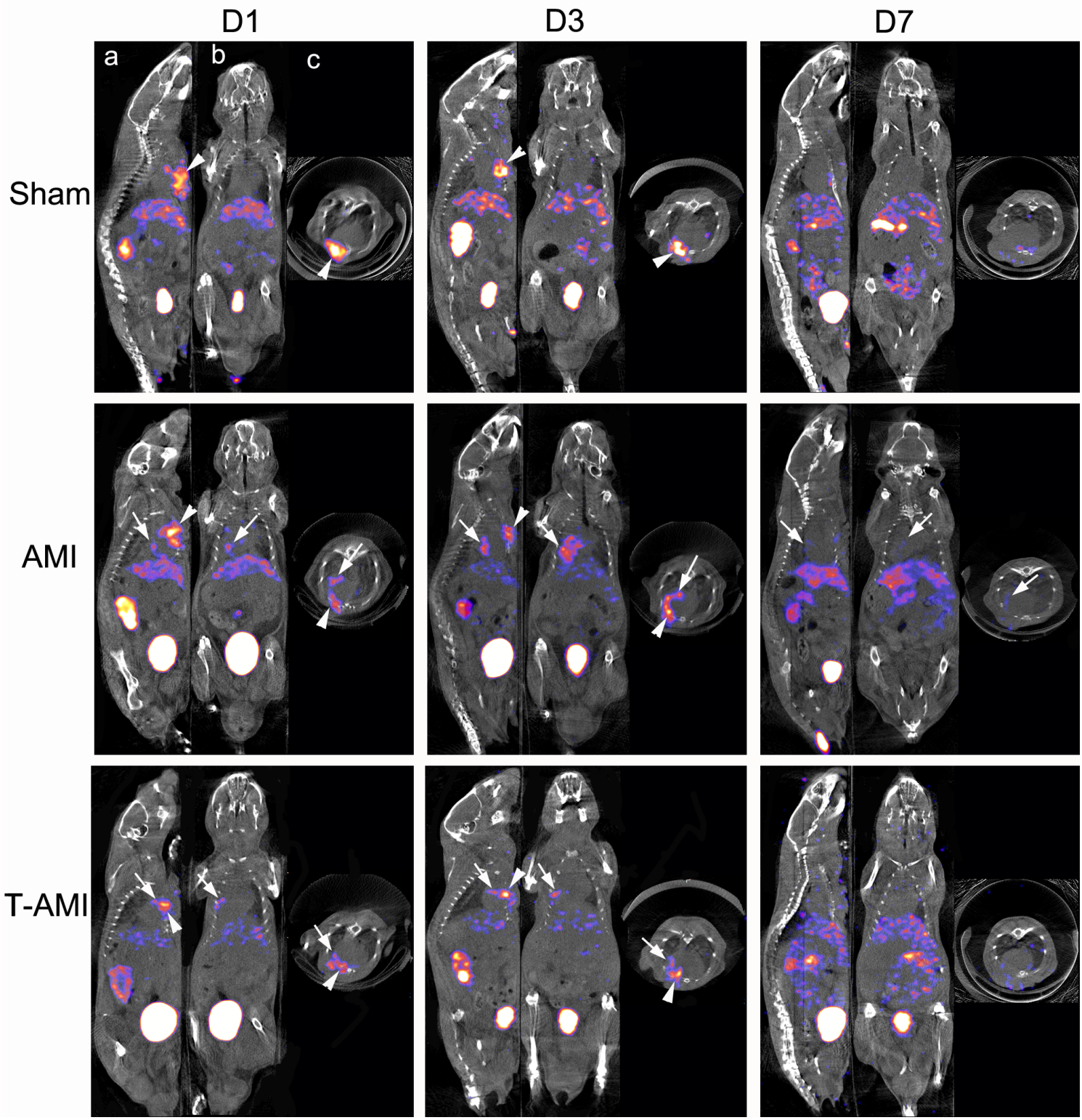

Figure 3

The in-vivo imaging of 99mTc-Duramycin SPECT/CT for non-invasively monitoring myocardial cell apoptosis in a mouse model of acute myocardial infarction and assess anti-apoptosis effect of atorvastatin. a, Micro-SPECT/CT sagittal images. b, Micro-SPECT/CT coronal images. c, Micro-SPECT/CT

axial images. The white arrow represented the uptake of 99mTc-Duramycin in myocardial death, and the white triangle displayed the uptake of 99mTc-Duramycin in death of thoracic surgical area.

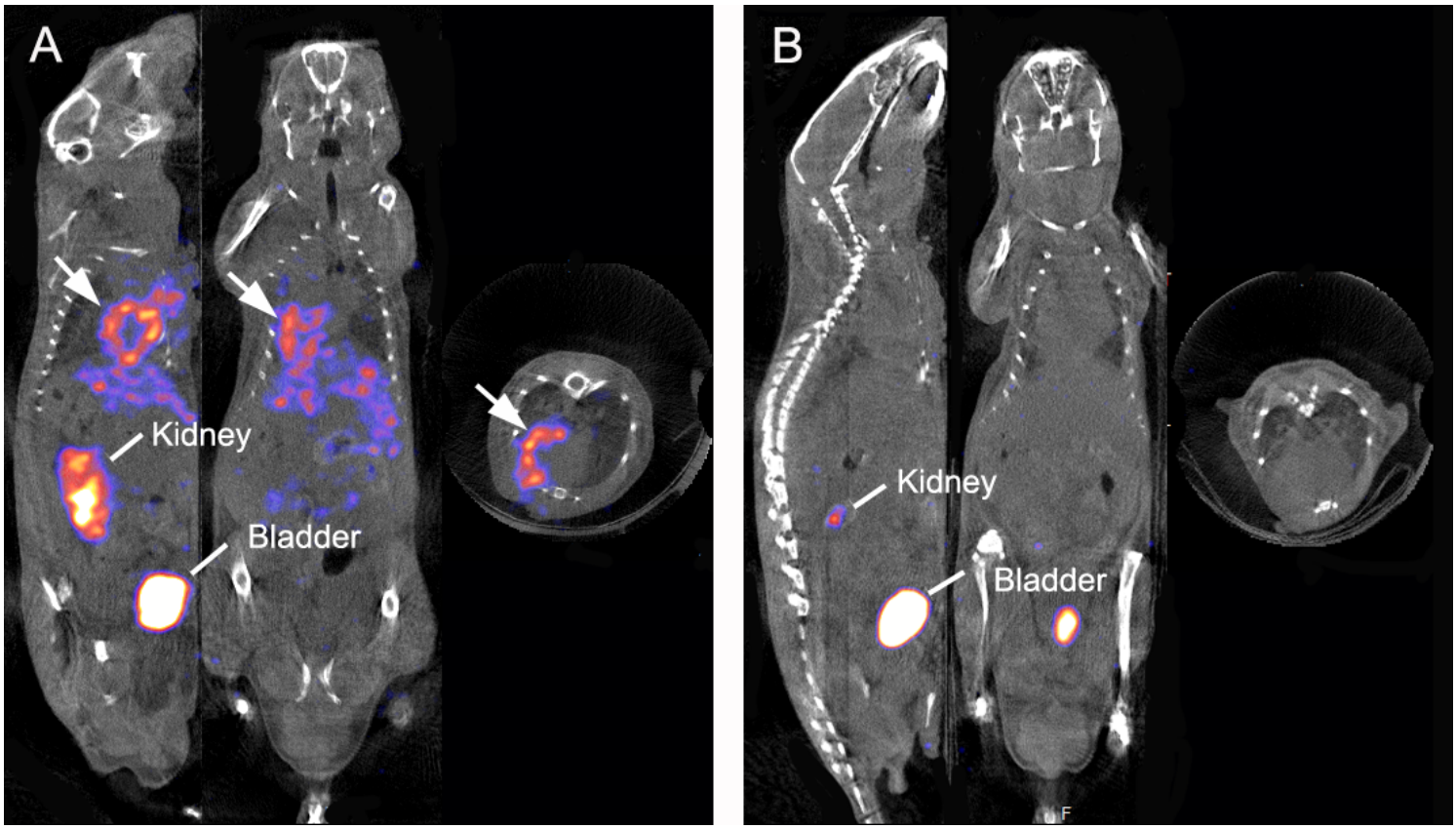

Figure 4

The 99mTc-duramycin (A) and 99mTc-linear-duramycin (B) of micro-SPECT/CT images in the AMI group. The white arrow represented the uptake of 99mTc-Duramycin in myocardial death.

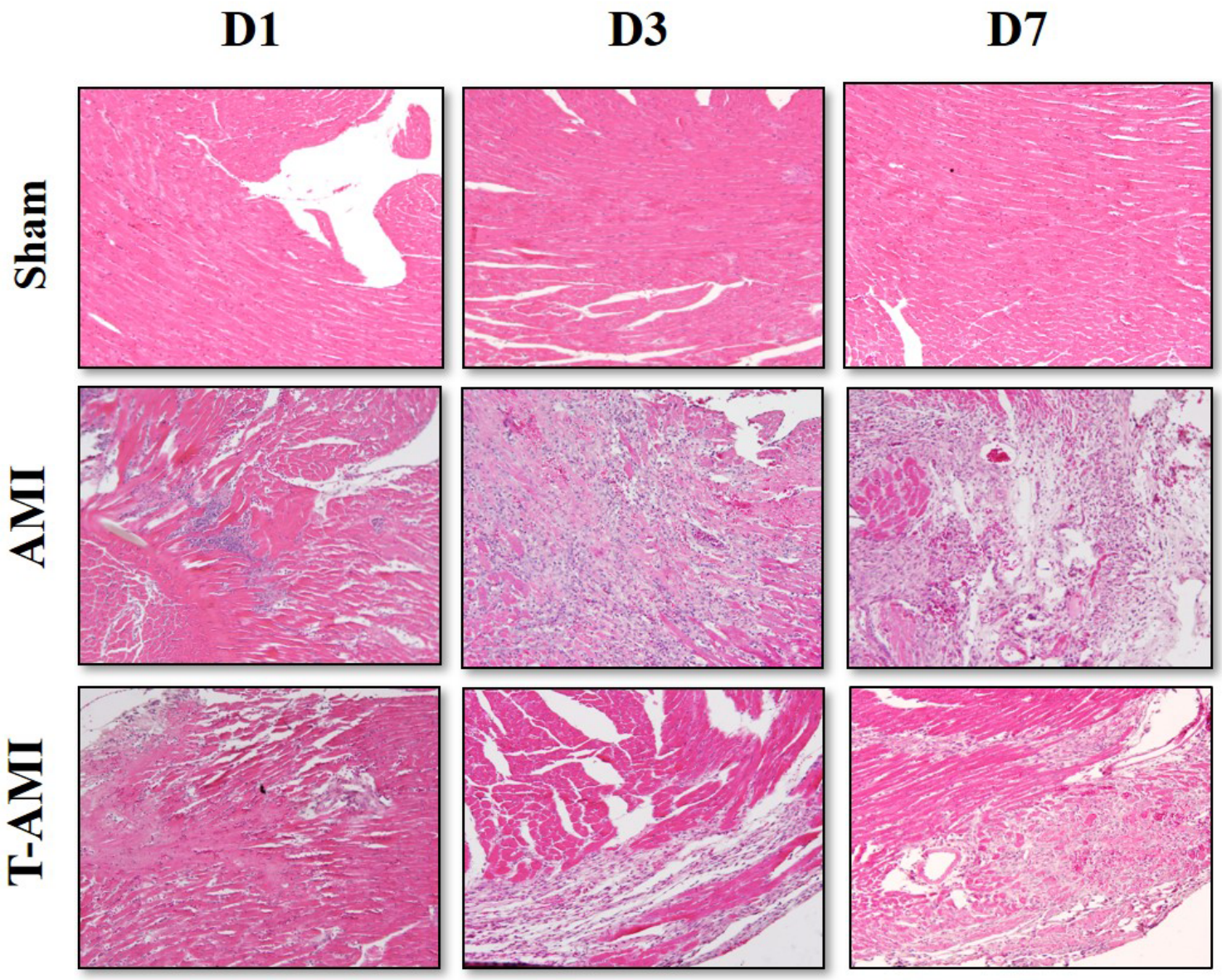

Figure 5

Histological analysis of myocardium injury after myocardial infarction. Representative H.E staining images of infarcted heart of the AMI and T-AMI group mice on D1, D3 and D7. Numerous immune cells, necrotic myocardial cells, loss of muscle fiber integrity and fibrosis were seen on D1, D3 and D7 post-MI compared to those in sham group. Atorvastatin attenuate the myocardial injury after MI for decreasing number of immune cells and necrotic myocardial cells.

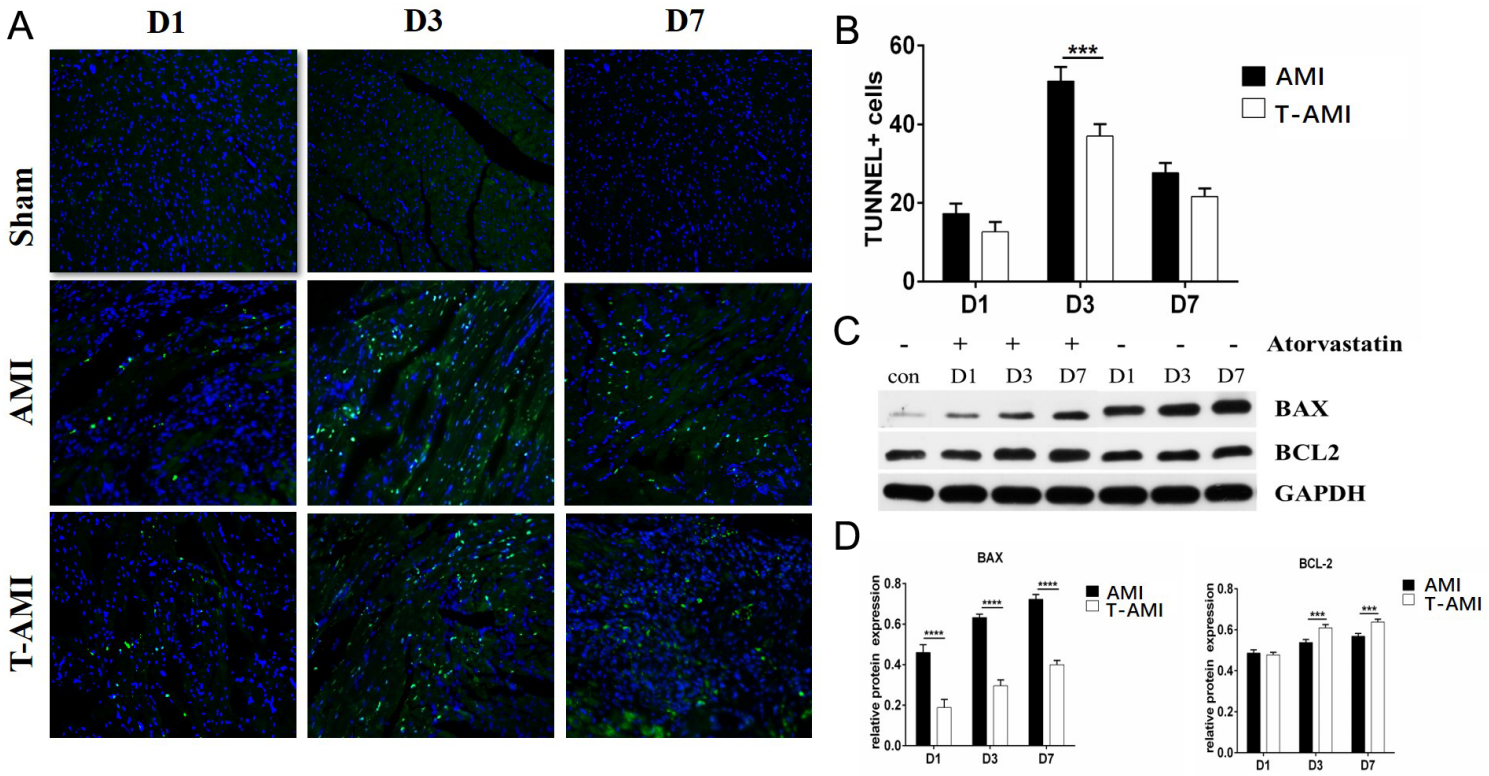

Figure 6

Evaluation of myocardial cells apoptosis after myocardial infarction. (A) Representative TUNEL staining images of infarcted heart of the AMI and T-AMI group mice at D1, D3 and D7. (B) Quantitation of TUNNEL+ cells in infarcted heart of the AMI and T-AMI group mice at D1, D3 and D7 after ligation. (C) Western blot analysis of BCL-2 and BAX in infarcted heart from the AMI and T-AMI group mice at D1, D3 and D7. The results from independent preparations are shown. (D) Protein levels of BCL-2 and in infarcted heart at D1, D3 and D7 were quantified by Image J software. *P < 0.05, **P < 0.01, ***P < 0.001, ****P < 0.0001, error bars represent the mean ± SD.